Simultaneous retrieval of aerosol refractive index and particle size distribution from ground-based measurements of direct and scattered solar radiation

Peter Romanov, Norman T. O'Neill, Alain Royer, and Bruce L. J. McArthur

Ground-based sunphotometer observation of direct and scattered solar radiation is a traditional tool for providing data on aerosol optical properties. Spectral transmission and solar aureole measurements provide an optical source of aerosol information, which can be inverted for retrieval of microphysical properties (particle size distribution and refractive index). However, to infer these aerosol properties from ground-based remote-sensing measurements, special numerical inversion methods should be developed and applied. We propose two improvements to the existing inversion techniques employed to derive aerosol microphysical properties from combined atmospheric transmission and solar aureole measurements. First, the aerosol refractive index is directly included in the inversion procedure and is retrieved simultaneously with the particle size spectra. Second, we allow for real or effective instrumental pointing errors by including a correction factor for scattering angle errors as a retrieved inversion parameter. The inversion technique is validated by numerical simulations and applied to field data. It is shown that ground-based sunphotometer measurements enable one to derive the real part of the aerosol refractive index with an absolute error of 0.03–0.05 and to distinguish roughly between weakly and strongly absorbing aerosols. The aureole angular observation scheme can be refined with an absolute accuracy of 0.15–0.19 deg. Offset corrections to the scattering angle error are generally found to be small and consistently of the order of −0.17. This error magnitude is deduced to be due primarily to nonlinear field-of-view averaging effects rather than to instrumental errors. © 1999 Optical Society of America

OCIS codes: 280.1100, 010.1100, 010.1110.

1. Introduction

Aerosol particles influence radiative transfer and photochemical mechanisms in the atmosphere and play a fundamental role in cloud formation processes.[1] They also determine to a certain extent the radiative and heat balance of the Earth-atmosphere system.[2] Interaction of aerosol particles with incoming and reflected solar radiation influences the quality of remotely sensed images of the Earth's surface from satellite-based and airborne platforms.[3] Understanding the direct influence of aerosols on the radiative transfer processes requires knowledge of the optical properties of the aerosols, such as extinction coefficient, phase function, and single scattering albedo, or in turn of their microphysical properties, such as size distribution and the refractive index that determine the aerosol optical features.

Ground-based sunphotometry is known to be a simple and reliable tool for monitoring column-integrated composition and optical properties of the atmospheric aerosol. Two methods are widely used in aerosol remote sensing: (1) the measurement of the direct solar radiation transmitted through the atmosphere (atmospheric transmission or extinction method) and (2) the measurement of the solar radiation scattered at near-forward directions (aureole or scattering method). In general, the information content of the extinction and scattering measurements

When this research was performed, P. Romanov, N. T. O'Neill, and A. Royer were with the Centre d'Applications et de Recherches en Télédétection, Université de Sherbrooke, Sherbrooke, 2500 Boulevard de l'Université, Sherbrooke, Quebec J1K 2R1, Canada. P. Romanov is now with the Office of Research and Applications, National Oceanic and Atmospheric Administration, National Environmental Satellite, Data, and Information Service, 5200 Auth Road, WWB 712, Camp Springs, Maryland 20746. His e-mail address is promanov@nesdis.noaa.gov. N. T. O'Neill is now with NASA Goddard Space Flight Center, Code 923, Greenbelt, Maryland 20746. L. J. B. McArthur is with the Atmospheric Environment Service, 4905 Dufferin Street, Downsview, Ontario M3H 5T4, Canada.

Received 14 May 1999; revised manuscript received 11 August 1999.

0003-6935/99/367305-16$15.00/0

© 1999 Optical Society of America

with respect to the aerosol physical characteristics is different. A number of studies have combined transmission and aureole measurements to exploit these different types of contribution and to improve the information properties of the observations.[4–8]

The availability of multispectral measurements of aerosol optical depth performed in visible and in near-infrared spectral ranges in addition to multispectral and multiangle measurements of the aerosol phase function at near-forward directions permits the inference of the aerosol particle size distribution $n(r)$ and the aerosol complex refractive index $m = \eta - i\chi$ and as a consequence the derivation of other aerosol physical and optical features that depend on $n(r)$, η, and χ. Numerous approaches to and methods of inversion of optical remote-sensing data were developed during the past few decades.[9–16] Most of these techniques are focused on the retrieval of only the aerosol size spectra and do not consider the influence (or the inversion opportunities) of variations in the refractive index. Some studies employed a simplified approach to the retrieval of the refractive index involving library methods or trial inversions of the optical measurements with different refractive indices (see, for example, Refs. 17–19). In these studies the values of the optical constants that minimize the residuals between the measured and the simulated radiances are taken to be the exact solution. It is obvious that the latter technique is time consuming and does not easily provide objective estimates of the retrieval accuracy of the refractive index.

The lack of a well-developed method to determine the aerosol refractive index can be explained as follows: First, the realistic variation of the optical constants of the atmospheric aerosol affect the aerosol extinction and the small-angle scattering to a lesser extent than the variation in the particle size distribution, and hence, if the measurement accuracy is not high, the refractive-index effects cannot be distinguished from the measurement noise. Second, the inclusion of the optical constants in the inversion procedure requires the calculation of the derivatives of the aerosol optical characteristics with respect to the real and imaginary parts of the refractive index. However, the optical constants enter into the Mie expressions for the aerosol extinction, scattering, and phase function in a complicated nonlinear way (see Ref. 20), thus hampering the development of the algorithm for the calculation of these derivatives.

The other common feature of the known approaches to the interpretation of the solar aureole measurements is the assumption that the scattering angles of aureole observations are known precisely. However, certain indeterminacy in the scattering angles may always exist because of the inaccuracies in the instrument angular positioning and Sun pointing. The error that results from the neglect of the instrument offset can significantly influence the accuracy of the particle size distribution retrieval, especially the retrieval of the concentration of large particles.[21]

In an earlier paper[22] the technique for inferring the particle size distribution along with the refractive index from the spectral transmission measurements in the visible and the near infrared was developed and tested. To compute the derivatives of the aerosol optical characteristics with respect to the aerosol optical constants that are required in the inversion, the modified Mie code of Rozanov *et al.*[23] was used. In the present study, first we apply a similar approach to the interpretation of combined atmospheric transmission and solar aureole observations and derive a formulation for the simultaneous retrieval of the particle size spectra and the refractive index from these data. Second, we allow for a certain indeterminacy in the values of the solar aureole observation angles, which may occur as a result of inaccuracy in the instrument positioning and Sun pointing. The factor that corrects for possible inaccuracy in the determination of the aureole scattering angles is also included in the inversion scheme and is derived along with the aerosol parameters. We give a description of the technique, analyze the information content of the measurements with respect to the parameters sought, estimate the potential accuracy of their retrieval, and present the results of the application of the developed technique to numerical simulations and to actual sunphotometer observations.

2. Theory and Details of Computation

A. Spectral Transmission and Solar Aureole Model

The spectral transmission technique is based on the formulation of Beer–Lambert law for the extinction of the solar radiation in the atmosphere:

$$E(\lambda) = E_0(\lambda)\exp[-m_0\tau(\lambda)], \tag{1}$$

where $E(\lambda)$ is the measured ground-based solar irradiance at wavelength λ, $E_0(\lambda)$ is the extraterrestrial solar irradiance, m_0 is the optical air mass [$m_0 = 1/\cos(\theta_s)$ for solar zenith angles $\theta_s \leq 75°$], and $\tau(\lambda)$ is the total optical thickness of the atmosphere. The spectral aerosol optical thickness $\tau_a(\lambda)$ is given by

$$\tau_a(\lambda) = \tau(\lambda) - \tau_R(\lambda) - \tau_g(\lambda), \tag{2}$$

where $\tau_R(\lambda)$ is the Rayleigh scattering optical thickness and $\tau_g(\lambda)$ is gaseous absorption.

The solar aureole is commonly defined as the region of enhanced brightness within approximately 15–20° of the solar disk.[10,24] A basic assumption of the solar aureole technique is that the forward peak of the phase function of the scattered solar radiation is controlled largely by single-scattering processes. This aureole feature allows one to simplify the physical model significantly and to approximate the effects of multiple scattering and surface contribution with a second-order corrective factor to the formal single-scattering solution of the radiative transfer equation[8,10,25]:

$$I_s(\Omega, \lambda) = m_0 E_0(\lambda)\exp[-m_0\tau(\lambda)][\tau_R(\lambda)P_R(\Omega, \lambda) + \tau_{sa}(\lambda)P_a(\Omega, \lambda) + \Delta_{ms}(\Omega, \lambda, A)], \tag{3}$$

where I_s is the aureole radiance measured at scattering angle Ω, $P_R(\Omega, \lambda)$ and $P_a(\Omega, \lambda)$ are the Rayleigh and aerosol phase functions, respectively, $\tau_{sa}(\lambda) = \tau_a(\Omega, \lambda)\omega_a(\lambda)$ is the aerosol scattering optical depth, $\omega_a(\lambda)$ is the aerosol single-scattering albedo, and $\Delta_{ms}(\Omega, \lambda, A)$ is a term that represents the contribution of the effects of multiple scattering and reflection from the surface in the solar aureole.

For aureole measurements acquired in the solar almucantar one can adopt the Box–Deepak[10] approximation for the multiple-scattering contribution:

$$\Delta_{ms}(\Omega, \lambda, A) = \tau_A(\lambda, A)P_R(0°, \lambda) + P_R(\Omega, \lambda)t_{ms}, \quad (4)$$

where

$$\begin{aligned} \tau_A(\lambda, A) &= A\tau_2/(1 - A\tau_3), \\ \tau_2 &= 1.34\tau_{ss}\cos\theta/[1.0 + 0.22(\tau_{ss}/\cos\theta)^2], \\ \tau_3 &= 0.9\tau_{ss} - 0.92{\tau_{ss}}^2 + 0.54{\tau_{ss}}^3, \\ t_{ms} &= 0.02\tau_{ss} + 1.2{\tau_{ss}}^2/(\cos\theta)^{1/4}, \\ \tau_{ss} &= \tau_R(\lambda) + \tau_{sa}(\lambda), \end{aligned} \quad (5)$$

A is the land surface hemispherical albedo, θ is the solar zenith angle, and τ_{ss} is the total scattering optical depth.

The aerosol particles were assumed to be homogeneous spheres. In general, the shape and composition of natural aerosol particles can be different from the properties assumed. The possible effect of the particle nonsphericity on the results of the study are discussed below. The adoption of the aerosol model mentioned above permits the application of spherical particle Mie theory to relate the aerosol optical properties to their microphysical properties. For a particle size distribution $n(r)$ the integrated Mie contributions are given by

$$\tau_a(\lambda) = \int_0^\infty \pi r^2 n(r) Q_{ext}(m, r, \lambda)\mathrm{d}r, \quad (6)$$

$$\tau_{sa}(\lambda) = \int_0^\infty \pi r^2 n(r) Q_{sca}(m, r, \lambda)\mathrm{d}r, \quad (7)$$

$$\begin{aligned} P_a(\Omega, \lambda) = \lambda^2/2\pi/\tau_{sa}(\lambda) \int_0^\infty n(r)[i_1(\Omega, m, r, \lambda) \\ + i_2(\Omega, m, r, \lambda)]\mathrm{d}r, \end{aligned} \quad (8)$$

where $m = \eta - i\chi$ is the complex index of refraction, $n(r)$ is the column integrated particle size distribution function [(number of particles/unit area)/unit size interval], $Q_{ext}(m, r, \lambda)$ and $Q_{sca}(m, r, \lambda)$ are the Mie extinction and scattering efficiency factors, respectively, and $i_1(\Omega, m, r, \lambda)$ and $i_2(\Omega, m, r, \lambda)$ are the Mie amplitude functions.

B. Formulation and Solution of the Inverse Problem

Equations (1)–(8) describe the relationship between aerosol microphysical properties and atmospheric transmission and solar aureole scattering as well as providing a formal basis for the inversion of the optical measurements to retrieve the aerosol characteristics. Following the ideas outlined above, we have developed a methodology for the simultaneous retrieval of the particle size distribution, the real and imaginary parts of the refractive index, and the factor that corrects for the nonzero offset angle of the instrument pointing toward the center of the solar disk. To specify the inverse problem we assumed that the sunphotometer data are available in the form of aerosol optical depth [Eq. (6)] derived from atmospheric transmission measurements in N spectral bands and aureole radiance [Eq. (3)] measured in M spectral bands at L scattering angles. Thus the total number of measurements input to the inversion procedure is $N + ML$. The measurement errors were assumed to be random. The particle size spectrum was specified as a volume distribution $v(r) = 4/3\pi r^3\, n(r)$ and represented in the form of a histogram of 20 logarithmically spaced size bins within a radius interval of 0.05–10 μm.. The aerosol particles were assumed to be represented by a fixed refractive index (independently of particle size and of the wavelength within the 0.38–1.02-μm spectral range).

We assumed that an error in the aureole observation scattering angles could occur as a result of a real or an effective constant offset in the instrumental pointing accuracy relative to the solar disk. For the two solar aureole scanning configurations that we employed, namely, almucantar and principal plane scans, this angular offset is approximately proportional to the scattering angle. Thus a correction factor for the scattering angle error (δ_Ω) was introduced as

$$\Omega_l = \Omega_l{}^* + \delta_\Omega, \qquad l = 1 \ldots L, \quad (9)$$

where $\Omega_l{}^*$ and Ω_l, respectively, represent noncorrected and corrected sets of scattering angles employed in the aureole observations.

For the inversion we assumed that all other atmospheric properties that could influence the radiative transfer within the 0.38–1.02-μm spectral were known. As well, we assumed a simplistic nominal value for the surface albedo to account for its second-order influence on measured sky radiances. The radiative transfer model that we used in this study included Rayleigh scattering and absorption by O_3 and NO_2 (calculated for the standard mid-latitude summer atmospheric model[26]). It was assumed that the atmospheric attenuation and solar aureole observations were performed outside any strong gaseous absorption bands. To specify the surface albedo we used the model of Cess and Vullis[27] for "pastureland." The spectral albedo value in this model is constant for wavelengths less than 0.7 μm ($A = 0.06$) and greater than 0.9 μm ($A = 0.43$) and increases linearly from 0.7 to 0.9 μm between these two extremes.

For the numerical inversion of the aerosol optical depth and solar aureole measurements we linearized Eqs. (3) and (6) and, accounting for the possible mea-

surement errors, reduced the problem to a set of equations of the form

$$\mathbf{F} = \mathbf{H}\phi + \varepsilon, \tag{10}$$

where $\mathbf{F}$ is the $(N + ML)$ column vector of the deviations of the measured aerosol optical thickness in N spectral channels and of the measured solar aureole radiance in M spectral channels at L angles from their mean values, ϕ is the column vector of the parameters to be determined, $\mathbf{H}$ is the matrix of partial derivatives of optical depth and solar aureole with respect to the unknown parameters, and ε is the column vector of the supposedly random and independent measurement errors

In the formulation of the inverse problem the column vector ϕ is defined by

$$\phi^T = \{\delta_{v1} \ldots \delta_{vK}, \delta_\eta, \delta_\chi, \delta_\Omega\}, \tag{11}$$

where $K = 20$, ϕ^T is the transpose of ϕ, δ_{vk} is the relative deviation of the particle volume concentration in the kth radius bin v_k from its mean value v_k*:

$$\delta_{vk} = (v_k - v_k^*)/v_k^*, \tag{12}$$

and δ_η and δ_χ are, correspondingly, the deviations of the real and the imaginary parts of the refractive index from their means. The total number of unknowns subject to the retrieval from the optical measurements comprised 23.

It should be noted that the linearization of Eqs. (3) and (6) with respect to the variables to be retrieved and the computation of the elements of matrix $\mathbf{H}$ is a rather straightforward procedure, except for the computation of the complex refractive index and the offset angle; the linearization process requires knowledge of the partial derivatives of the aerosol optical characteristics $[\partial\tau_a(\lambda)/\partial\eta,\ \partial\tau_a(\lambda)/\partial\chi,\ \partial P_a(\Omega, \lambda)/\partial\eta,\ \partial P_a(\Omega, \lambda)/\partial\chi$, and $\partial P_a(\Omega, \lambda)/\partial\Omega]$. To obtain the derivatives of the optical parameters relative to η and χ we implemented the method devised by Rozanov *et al.*[23] A brief description of this algorithm as well as the technique that we used to compute the derivatives of the aerosol phase function with respect to the scattering angle are given in Appendix A.

The retrieval of the aerosol microphysical properties from the optical sounding data is known to be an ill-conditioned inverse problem from the mathematical point of view.[4,15,24] In general this means that the solution may not be unique and that any experimental error in the measurements may be greatly amplified in the inversion of Eq. (10). In the absence of constraints the solution is accordingly highly unstable. To overcome these difficulties *a priori* information with respect to the unknowns must be introduced to allow for the solution stabilization (or regularization). The use of the *a priori* information on the unknowns is often viewed as supplementing the direct observations that alone lead to the ill-posed inverse problem, by virtual measurements.[28] The combination of the real and virtual measurements stabilizes the inversion procedure and thus effectively ensures that the problem is well posed. Several techniques for solving ill-posed inverse problems exist. The constrained linear inversion method was devised by Twomey[29]; Wark and Fleming[30] used empirical orthogonal functions for constraining the solution; a statistical approach to solution stabilization was developed by Turchin and Nozik,[31] Westwater and Strand,[32] and Rodgers.[33] Discussions and comparative analyses of these methods can be found in a number of published reviews (see, for example, Ref. 28).

The statistical characteristics of the measurement noise for remote-sensing techniques such as sunphotometry are typically known or can be estimated. Usually we also have certain *a priori* knowledge of the expected variability of the parameters that are being retrieved. Furthermore, it is quite reasonable to assume normally distributed probabilities for both the measurement errors and the unknowns sought. Given these conditions, the application of a statistical approach to the regularization of the solution for Eq. (10) is quite appropriate. In this case an optimum linear unbiased estimate of the unknown vector ϕ is[14,28,32]

$$\hat{\phi} = (\mathbf{H}^T\mathbf{\Sigma}^{-1}\mathbf{H} + \mathbf{D}^{-1})^{-1}\mathbf{H}^T\mathbf{\Sigma}^{-1}\mathbf{F}, \tag{13}$$

where $\mathbf{\Sigma}$ is the covariance matrix of measurement errors, which are assumed here to be random and independent, and $\mathbf{D}$ is the *a priori* covariance matrix of the unknown parameters. It should be noted that the elements of matrix $\mathbf{H}$ in Eq. (13) depend on the parameters sought [$v(r)$, η, χ, and Ω], and thus the inverse problem considered is nonlinear. That is why, in practice, one should use an iterative procedure to obtain the solution of Eq. (13). To perform the retrievals for numerical simulations and for the processing of field measurements we applied an algorithm analogous to the one developed by Dubovik *et al.*[13] This algorithm employs a Newton–Gauss iterative scheme and is based on a statistical estimate of the inverse problem solution at each step of the iteration.

One of the most straightforward and widely used methods to study the potential of ground-based remote-sensing data and to examine the reliability of the inversion scheme is numerical simulation of experiments within a closed scheme. This requires a simulation of the measurements, their degradation by the addition of noise, and the subsequent inversion of the degraded data. The foregoing approach often yields insight into the general capabilities of the remote-sensing measurements and in particular helps us to understand the influence of the initial guess on the results of the retrieval. However, it is difficult to obtain objective estimates of the retrieval accuracy because such estimates require numerous simulations over an ensemble of input measurements.

We can independently estimate the retrieval accuracy of the linear solution $\hat{\phi}$ given by Eq. (13) by

calculating the solution residual (or *a posteriori*) covariance matrix[28,32]:

$$\hat{\mathbf{D}} = \mathbf{D} - \mathbf{D}\mathbf{H}^T(\mathbf{H}\mathbf{D}\mathbf{H}^T + \boldsymbol{\Sigma})^{-1}\mathbf{H}\mathbf{D} \qquad (14)$$

or, alternatively,

$$\hat{\mathbf{D}} = (\mathbf{D}^{-1} + \mathbf{H}^T\boldsymbol{\Sigma}^{-1}\mathbf{H})^{-1}.$$

The square root of the $\hat{D}_{ii}$ element of matrix $\hat{\mathbf{D}}$ represents *a posteriori* variance of the ith unknown parameter and can be treated as an estimate of the accuracy of its retrieval. The ratio of the diagonal elements of the *a priori* and *a posteriori* covariance matrices characterizes the reduction in an *a priori* variance of the unknowns to be derived from the remote-sensing measurements and thus represents a measure of the information contained in the observations with respect to the corresponding aerosol parameters.[32]

The potential for retrieving aerosol microphysical properties from sunphotometer measurements is determined to a great extent by the particular spectral and angular scheme employed in the observations and by the instrument noise characteristics. In this study we analyzed simulated measurements and real observations acquired by the sun- and sky-scanning CIMEL CE-318 radiometer. Instruments of this type were used intensively in a number of recent atmospheric aerosol field experiments[21,34] and are employed to provide routine observations in the global aerosol robotic network[35] (AERONET) as well as in the Canadian branch of this network, AEROCAN.[36] A brief description of the instrument is given in Section 3 below. In Section 4 we examine the potential of the CIMEL sunphotometer measurements for providing information on aerosol properties (both the size spectra and the refractive index) and the possibilities for correcting errors in the aureole observation angles. In terms of simulations, both approaches to the analysis of the aerosol retrieval accuracy described above are investigated. First, in Subsection 4.A, we estimate accuracies through the computation of the solution residual covariance matrices [Eq. (14)]. Second, in Subsection 4.B, the peculiarities of the inversion scheme are studied in a series of numerical experiments, which include the simulation of sunphotometer measurements, their distortion by the modeled instrument noise, and the subsequent iterative retrieval of the aerosol properties.

3. Characteristics of the Instrument

The automatic sun–sky CIMEL radiometer can measure atmospheric spectral transmission and sky radiance in the almucantar and the principal plane. For the instruments employed in the AERONET, seven of the eight CIMEL filters (centered at 0.34, 0.38, 0.44, 0.50, 0.67, 0.87, and 1.020 μm) are used for aerosol remote sensing. The eighth spectral filter is centered at 0.94 μm and is used to derive total precipitable water. The sky-scanning measurements are performed with four filters, centered at 0.44, 0.67, 0.87, and 1.02 μm. These measurements (of which the aureole measurements employed in our inversions were a subset) are acquired with a 1.8° full angle field of view in variable angular steps that increase with the increase of the angular distance from the center of the solar disk. The angular schemes of the sky radiance measurements in the almucantar and the principal plane are presented in Table 1. It is seen that the most detailed sky scanning is carried out in the solar aureole range (2°–20° from the Sun), where the angular increments between measurements vary from 0.5° to 2°.

Table 1. CIMEL Sky-Scanning Angular Schemes

Measurement Type	Angular Scan Scheme[a] (°)
Principal plane	2 (0.5) 4 (1) 6 (2) 20 (5) 50 (10) 140
Almucantar	2 (0.5) 4 (1) 6 (2) 20 (5) 50 (10) 100 (20)

[a]The numbers outside the parentheses represent the values of the reference angles; the numbers within parentheses represent the angular increments that we used to scan between two neighboring reference angles.

The aerosol optical depths derived from the atmospheric transmission observations are reported to have maximum errors of ±0.01, whereas the absolute uncertainty of the sky radiance measurements is estimated to be ~5% (see Ref. 35). Stray-light rejection allows for reliable aureole measurements at angles greater than 3° from the center of the solar disk. An automatic Sun-pointing and -tracking scheme is programmed through microprocessor control of an altazimuth drive. The errors in the instrument positioning and Sun pointing in some cases may be as large as half of a degree.[21]

4. Analysis of the Retrieval Accuracy of the Size Spectra and the Aerosol Refractive Index

A. Retrieval Accuracy Estimates Based on the Residual Covariance Matrix Calculations

The estimation of the retrieval accuracy through the calculation of the *a posteriori* covariance matrix [Eq. (14)] requires a predetermination of the statistical characteristics of the expected solution and the measurement noise statistics (matrices $\mathbf{D}$ and $\boldsymbol{\Sigma}$, respectively). To specify the $\mathbf{D}$ matrix we assumed 100% uncertainty in the *a priori* determination of the particle concentration in each of the 20 histogram size bins. The uncertainties in the real and the imaginary parts of the refractive index were assumed to be 0.1 and 0.005, respectively, and the sky-scanning pointing error was taken equal to 0.25°. The spectral bands of the simulated transmission measurements were those of the AERONET CIMEL sunphotometers, with the exception of the short-wave channel centered at 0.34 μm. This channel was excluded from consideration because of suspected calibration problems. The aureole observation scheme employed for the numerical retrievals was based on the spectral and scanning configuration of AERONET instruments: 10 angular measurements

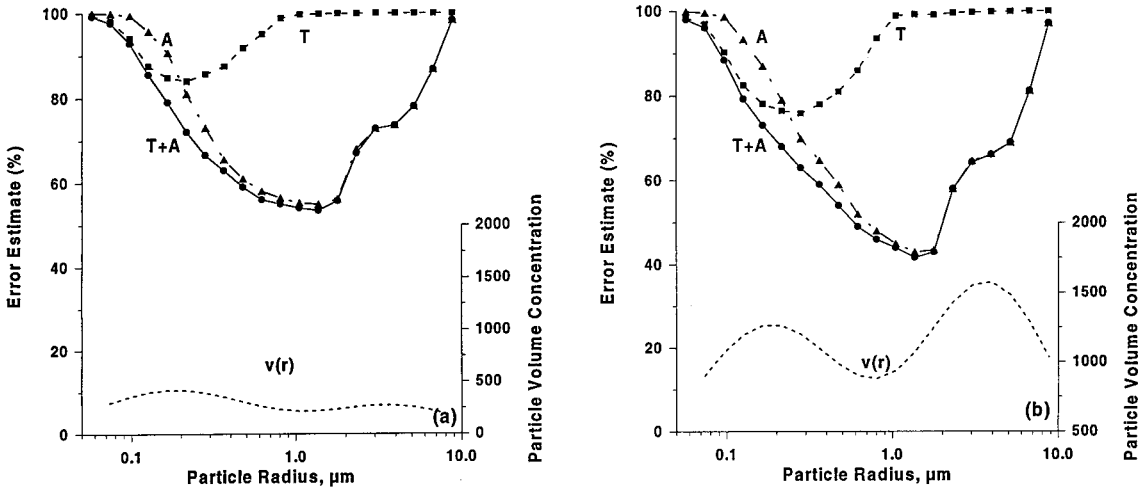

Fig. 1. Aerosol size distribution retrieval error estimates for different schemes of sunphotometer measurements (T is for the transmission measurements, A is for the aureole measurements, and T + A is for the combined aureole and transmission measurements.) The results are presented for (a) the turbid and (b) the clear aerosol models. The accuracies of measurements of optical depth and the solar aureole were assumed equal to 0.01 and 5.0%, respectively. Volume concentration is given in units of $(cm^3/cm^2)/\mu m \times 10^9$.

spaced according to Table 1 in intervals of 3°–16° from the Sun's center and acquired in the four spectral channels mentioned above. The measurement errors were considered to be independent and normally distributed for both the transmission and the aureole observations. The solar zenith angle in the calculations was assumed to be 30°.

Two aerosol models, representing clear and turbid atmospheric conditions, were used in the calculation of the residual error covariance matrices. The particle size distribution for both aerosol models consisted of accumulation and coarse modes identical to the standard water-soluble and sea-saltlike aerosol size spectra models of McClatchey *et al.*[26] The particular shape of a particle size distribution was defined by the volume ratio of the accumulation to coarse mode (0.2 for the clear model and 1.0 for the turbid model), and the total aerosol concentration was normalized to provide aerosol optical depths at 0.5-μm wavelength equal to 0.05 and 0.2 for the clear and the turbid models, respectively. The particles were assumed homogeneous and isotropic with a refractive index of $1.50 - i0.005$ in the spectral range 0.38–1.020 μm.

It is well known that the information content of the spectral optical depth and solar aureole measurements, which is characterized in this paper by the *a priori* variance reduction of the retrieval unknowns, is different in different radius regimes of the particle size distribution. Atmospheric spectral transmission is more sensitive to variations in small-particle concentrations, whereas aureole measurements are more informative with respect to large-particle concentrations.[5] Estimates of size spectra retrieval accuracy that were computed from the residual covariance matrix [Eq. (14)] for sunphotometer simulations based on the two aerosol models described are presented in Fig. 1. In general, our estimates are consistent with results reported in the literature. Solar aureole and transmittance measurements provide almost equal retrieval errors for particles within the 0.19–0.25-μm radius interval. The size spectra of aerosol particles in the smaller and larger radius ranges can be more accurately retrieved with the transmission and aureole measurements, respectively. Figure 1 also shows that aureole observations performed with the CIMEL instrument provide much higher particle spectra retrieval accuracy. This effect is partly attributable to the fact that the total number of aureole observations exceeds the number of optical depth measurements by more than a factor of 5. There is, to be sure, considerable redundancy in the 40-odd measurements that constitute a single scan; i.e., some of them contain almost no new information on the aerosol characteristics in terms of independent pieces of information as defined by Twomey and Howell.[15] However, measuremental redundancy in the retrieval scheme reduces the effects of measuremental noise and thus has a positive effect on the retrieval accuracy.[32]

An increase in aerosol loading results in an improvement in the size distribution retrieval accuracy [compare Figs. 1(a) and 1(b)]. However, even for a turbid aerosol model the estimated precision of particle concentration reconstruction by use of the combined transmission and aureole measurements is not high: The smallest error estimates in the 0.1–8-μm particle radii range are 40%.

As can be seen from Table 2, the *a priori* knowledge of ±0.1 in the real part of the refractive index can be significantly improved by use of ground-based sunphotometer observations. Solar aureole measurements contain more information on aerosol optical constants than do pure spectral optical depth measurements; the combined scheme yields turbidity-dependent retrieval accuracies of 0.033–0.047 for the real part of the refractive index (given typical errors for these types of observation; i.e., 0.01 for optical

Table 2. Estimates of the Retrieval Accuracy of the Aerosol Refractive-Index and Scattering-Angle Corrective Factor for Separate Measurements of Atmospheric Transmission, of Solar Aureole, and of Combined Transmission and Aureole[a]

		Uncertainty			
			a posteriori		
Aerosol Model	Parameter	*a priori*	Transmission	Aureole	Transmission + Aureole
Turbid	η	0.1	0.084	0.046	0.033
	χ	0.005	0.005	0.0048	0.0042
	$\Delta\Omega$ (°)	0.25	0.250	0.151	0.147
Clear	η	0.1	0.086	0.056	0.047
	χ	0.005	0.005	0.0049	0.0047
	$\Delta\Omega$ (°)	0.25	0.250	0.187	0.185

[a]The accuracies of the optical depth and solar aureole measurements were assumed equal to 0.01 and 5.0%, respectively.

depth and 5% relative error for the solar aureole radiance). Aureole measurements provide marginally more information on the imaginary part of the refractive index (see χ in Table 2), and only a slight improvement (i.e., reduction in the *a posteriori* variance relative to the *a priori* variance) in the knowledge of the atmospheric aerosol absorbing properties could be expected. In particular, if the combined aureole and spectral transmission measurements are employed, the assumed *a priori* uncertainty of 0.005 in χ decreases to 0.0042–0.0047, depending on the aerosol model considered. The incorporation of an angular correction term in the inversion improves the geometrical accuracy of the aureole observations. The *a priori* variance of 0.25° in the observation scattering angle can be reduced to 0.15°–0.19°.

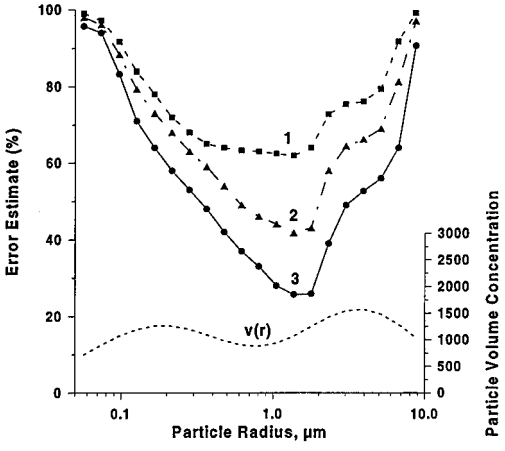

Fig. 2. Influence of measurement errors on the accuracy of the particle size distribution retrieval. Curve 1, $\varepsilon_t = 0.02$, $\varepsilon_a = 10\%$; curve 2, $\varepsilon_t = 0.01$, $\varepsilon_a = 5.0\%$; curve 3, $\varepsilon_t = 0.005$, $\varepsilon_a = 2.5\%$. ε_t and ε_a are the transparency and the solar aureole measurement errors, respectively. The turbid aerosol model was used. Volume concentration is given in units of $(cm^3/cm^2)/\mu m \times 10^9$.

The accuracy of remote-sensing measurements is one of the principal factors that determine the information content of the measurements and hence their potential for use in deriving aerosol properties. The results given in Fig. 2 and Table 3 indicate what level of retrieval accuracy could be expected if the measurement precision varied. It can be seen that an increase by a factor of 2 in the precision of the aureole and transmission measurements results on average in a 10–20% decrease in the errors of the size distribution retrieval. For sunphotometry errors greater than or equal to typical values (0.01 and 5%) the information retrieval potential of the imaginary part of the refractive index is marginal, whereas useful information on the real part of the refractive index can still be extracted even if the accuracy of the measurements is significantly degraded. In the case of the greatest measurement precision considered in the simulation studies (0.005 for the optical depth and 2.5% for the aureole) the retrieval accuracies of the real and the imaginary parts of the refractive index were 0.022 and 0.0034, respectively, whereas the precision of the angular corrective factor was better than 0.1°. It should be noted that this measurement accuracy was specified as a requirement for the aerosol monitoring supersites to be organized in the future.[37]

Table 3. Influence of the Measurement Errors on the Retrieval Accuracy Estimates[a]

		Uncertainty		
		a posteriori		
Parameter	*a priori*	$\varepsilon_t = 0.005$, $\varepsilon_a = 2.5\%$	$\varepsilon_t = 0.01$, $\varepsilon_a = 5.0\%$	$\varepsilon_t = 0.02$, $\varepsilon_a = 10\%$
η	0.1	0.022	0.033	0.048
χ	0.005	0.0034	0.0042	0.0046
$\Delta\Omega$ (°)	0.25	0.095	0.147	0.196

[a]Combined transmission and solar aureole measurements are used. ε_t and ε_a are the atmospheric transmission and aureole measurement errors, respectively. The turbid aerosol model was used to yield these results.

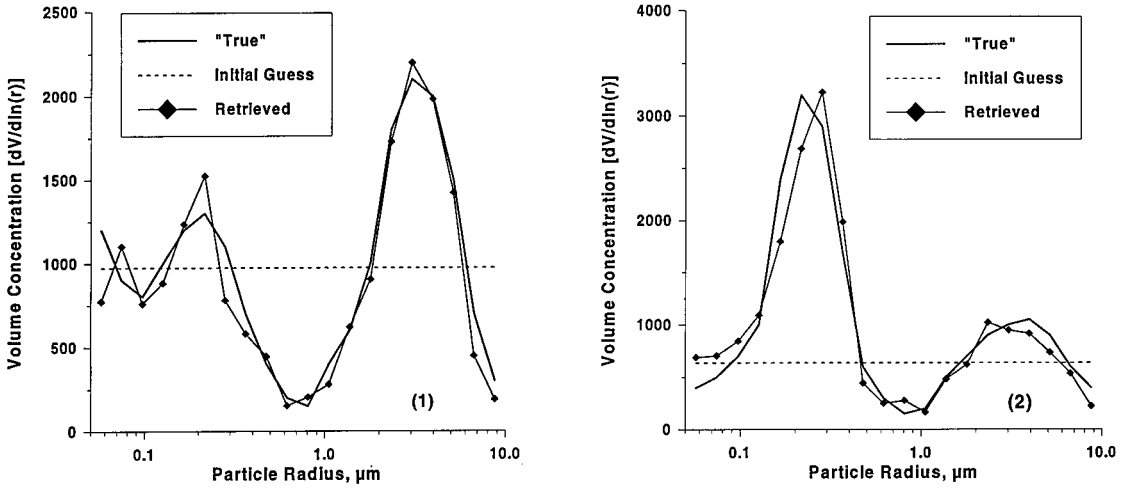

Fig. 3. Two examples of aerosol size distribution retrieval. Volume concentration is given in units of $(cm^3/cm^2)/\mu m \times 10^9$.

The error analysis presented above contains several simplifications and accounts for only part of the factors that hamper the retrievals. The problem was considered in a linear approach: The statistics used were assumed to be correct, and the error estimates obtained were treated as independent; thus potentially nonzero, nondiagonal elements of the residual covariance matrix were not considered. Obviously these estimates may be considered only as preliminary and approximate. More-objective estimates of the retrieval accuracy can be obtained by use of another traditional approach for investigating remote-sensing problems: the simulation of real measurements that have been degraded by measurement errors (simulated by a noise model) and the subsequent inversion of these data. This approach is time consuming but gives a better understanding of how particular remote-sensing measurements can provide information on specific aerosol properties. Results from the application of this approach to simulated sunphotometer measurements are presented in the following subsection.

B. Inversion of Simulated Sunphotometer Measurements

As we pointed out above, the inverse problem that begins with the formulation given in Eq. (10) and that consists in a size distribution and refractive-index retrieval from optical measurements is nonlinear. Thus the obvious approach to the solution of this inverse problem is to employ an iterative procedure. To recover the unknown vector ϕ from the simulated as well as real spectral transparency and solar aureole measurements we used a Newton–Gauss iterative scheme based on the statistical estimation approach[13]:

$$\phi_{t+1} = \phi_t - (\mathbf{H}_t^T \boldsymbol{\Sigma}^{-1} \mathbf{H}_t + \mathbf{D}^{-1})^{-1} (\mathbf{H}_t^T \boldsymbol{\Sigma}^{-1} \mathbf{F}_t + \mathbf{D}^{-1} \phi_t), \tag{15}$$

where ϕ_t, $\mathbf{H}_t$, and $\mathbf{F}_t$ are, respectively, the solution estimate, matrix $\mathbf{H}$, and vector $\mathbf{F}$ at the tth iteration step. The variations of ϕ were constrained in the inversion to avoid physically meaningless values of retrieved parameters. The iterative procedure was terminated when the mean-square residual difference between measured and modeled aureole radiance and optical depths was less than the prescribed level of measurement noise (otherwise the maximum number of iterations was set equal to 10). In all the retrievals we used a simple initial guess of a constant volume size distribution in the 0.05–10-μm radius range $[v(r) = dV/d\log(r) = c]$. This is equivalent to a Junge-type number distribution $n(r) = br^{-a}$, with $a = 4$. The particular value of c used in the inversion was determined such that the first-guess aerosol optical depth was equal to the measured optical depth at 1.02 μm. The initial-guess value of the aerosol complex refractive index was taken to be equal to $1.50 - i0.01$. It will be remembered that in the numerical experiments all other atmospheric and land surface properties aside from those specified in vector ϕ of Eq. (11) were not retrieved but rather were assumed to be known *a priori*.

Numerous experiments that modeled sunphotometer observations and their subsequent inversions have been conducted to investigate the performance of the inversion scheme and to study the accuracy of the retrieved aerosol properties. Although it is hardly possible to consider all conceivable states of the atmospheric aerosol, we believe that the simulated experiments carried out provided a good basis for understanding the potential and limitations of the atmospheric transmission and solar aureole measurements with respect to the retrieval of aerosol properties by means of the inversion developed in this paper. The performance of the inversion scheme and its provision of robust and accurate retrievals for two completely different aerosol types are illustrated in Fig. 3 and Table 4. In the first example the inversion scheme was applied to the case of a predominantly dustlike aerosol with a pronounced coarse mode and a refractive index of $1.65 - i0.02$. The second example shows the retrieval results for an aerosol with a strong accumulation mode and a re-

Table 4. Retrievals of the Optical Constants and Angular Corrective Factor in the Numerical Simulations[a]

Case Number	Parameter	True Value	Initial Guess	Retrieved Value
(1)	η	1.65	1.50	1.68
	χ	0.020	0.010	0.017
	$\Delta\Omega$ (°)	−0.30	0.00	−0.36
(2)	η	1.35	1.50	1.36
	χ	0.000	0.010	0.002
	$\Delta\Omega$ (°)	0.30	0.0	0.39

[a]Cases (1) and (2) correspond to the retrievals of particle size distribution illustrated in Fig. 3. Combined transmission and solar aureole measurements were used.

fractive index of $1.35 - i0.0$. In both cases a substantial shift in the values of scattering angles for the measured aureole was simulated to test the sensitivity of the inversion results to instrument positioning errors relative to the solar disk (−0.3° in the first example and 0.3° in the second one). The spectral and angular observation scheme employed in the numerical experiments was the same as that used above for the residual error calculations. Normally distributed measurement errors with standard deviations of 0.01 and 5% in optical depth and aureole radiance, respectively, were modeled with a random-number generator.

It can be seen in both examples in Fig. 3 that the retrieved size distribution closely follows the true $v(r)$ in the coarse-particle mode size range ($r > 1.0$ μm). Although the accumulation mode results ($r = 0.1$ to $r = 0.5$ μm) are less accurate, the maximum $v(r)$ retrieval errors even for this size range do not exceed 36%. The lack of optical sensitivity to particles with radii less than 0.1 μm results in the decreased retrieval accuracy.

Although in both examples the true values of the optical constants were significantly different from the first-guess values, the inversion provided good retrieval accuracy for the real part of the refractive index and properly corrected the value of the absorption coefficient χ (see Table 4). The retrieval errors of η were 0.03 and 0.01 in the two simulations, whereas the corresponding errors in χ were equal to −0.003 and 0.002. In both examples the inversion procedure produced an accurate correction (within 0.09°) to the offset in scan angle.

The accuracy of the aerosol parameter retrieval in the numerical experiments is coherent with the retrieval error estimates from the error covariance matrix calculations above. However, in some cases the accuracy of the numerical experiments was slightly better than the accuracy obtained for the error covariance matrix calculations. The probable reason for this is that the first-guess particle size distribution fitted from the transmission measurements in the numerical experiments was closer to the true size distribution than the first guess assumed in the residual error covariance matrices calculation. In the two numerical experiments of Figs. 3(a) and 3(b), the absolute (size-range averaged) differences between the first-guess size distribution and the true size distribution were 87% and 46%, respectively. In contrast, the *a priori* uncertainty in particle concentrations assumed in the error covariance matrix calculations was 100%. The results from both methods demonstrate the potential for retrieving the refractive index and the particle size distribution from ground-based sunphotometer measurements. The retrieval accuracy of the real part of the refractive index (0.03–0.05) estimated for the rough first guess for the aerosol size distribution used is in agreement with the results presented by Weindisch and von Hoyningen-Huene,[18] who used an instrument with spectral characteristics similar to those of the CIMEL sunphotometers. Using the aerosol optical depth data measured in the near-infrared spectral channel, we can obtain a better first guess for the particle size distribution and thus obtain a higher retrieval accuracy for η. In general, retrieval accuracy of the imaginary part of the refractive index is rather low (0.0042–0.0047). The improved first guess for the particle size spectra brought about through the use of the near-infrared channel yields only a slight improvement in the retrieval of χ. This means that inversion procedures applied to the combination of ground-based spectral transmission measurements and sky radiance measurements (limited to the solar aureole) are sensitive only to large changes in the absorption properties of the atmospheric aerosol.

5. Discussion of the Assumptions Made in the Study

Several assumptions and simplifications that were adopted in the aerosol and radiative transfer model require additional discussion. We also try wherever possible to estimate approximately the potential effect of these simplifications on the aerosol retrievals.

First and foremost, the idea that refractive index can be retrieved from transmission and aureole radiance measurements warrants discussion. If one derives the aerosol optical depth spectrum for a given refractive index and size distribution it is not difficult to demonstrate that one can obtain virtually equivalent optical transmission effects by decreasing the refractive index while simultaneously shifting the particle size distribution to larger values. This means that it would be difficult if not impossible to extract refractive index and particle size distribution simultaneously from transmission measurements alone. To complicate matters further, the aureole radiance is dominated by diffraction effects and hence is fairly insensitive to refractive index. The resolution of this apparent difficulty lies in the combination of the two types of data; the increase in particle size required for creation of the equivalent transmission effects to a decrease in refractive index constrains the computed aureole radiance. The particles are larger than they should be, and the phase function is thus more forward than it should be. Significant discrepancies between computations and the actual data will occur, and the combined inversion

routine will not be satisfied in its search for minimal error.

Aerosol particles in our study were assumed to be homogenous dielectric spheres. Particle sphericity is a typical assumption for the retrieval of aerosol properties from transmission and forward scattering optical measurements. The reasons for these assumptions are as follows: First, most of the nondust-like atmospheric aerosol particles are either liquid or liquid coated and thus can be well represented as spheres. Tropospheric dustlike particles are certainly of irregular shape, but their concentration and optical effects are usually small because of their predominantly large size and consequently high sedimentation rate. Second, the difference in the extinction cross section for spherical and nonspherical particles quickly decreases with the increase of particle size and becomes negligible at particle size parameter values as small as 12 (Ref. 38); these parameters are far less than the typical dustlike particle size parameters in the visible and near-infrared parts of spectrum. Modeling studies[38–40] suggest that the scattering phase function of nonspherical particles differs from the phase function of equivalent spheres. However, this difference is significant only for scattering angles larger than 60° (Ref. 40) and almost vanishes in the small-angle aureole region.[38] A similar conclusion was made by Kaufman *et al.*[37] and Nakajima *et al.*[41] based on *in situ* observations of atmospheric aerosol scattering properties. Thus it is believed that in general, even if nonspherical particles are present in the atmosphere, their effects on the measured atmospheric transmission and solar aureole would be hardly distinguishable from other parametric perturbations in aerosol properties and instrumental noise.

The consideration of spherical–nonspherical differences in particle optical properties by Pinnick *et al.*[42] and Nakajima *et al.*[41] led them to conclude that one can equate the scattering characteristics of a system of nonspherical particles with a spherical polydispersion of a total equivalent volume by assigning a large fictitious absorption index to Mie particles. The estimated magnitude of the required correction to the imaginary part of the refractive index varies from 0.02 and 0.12. This may be important for aerosol remote sensing inasmuch as it implies that the use of the spherical model in the inversion of optical measurements can result in an overestimate of the complex (absorption) part of the refractive index.

The refractive index in our study was considered to be independent of wavelength. In actual fact the real part of the refractive index for natural aerosol substances varies by 0.01–0.02 in the visible and near-infrared wavelength ranges.[26] This variability is, on the average, a factor of 2 less than the estimated error in the η retrieval for our sunphotometer measurements and thus can be neglected. This variability would be an issue only if the measurement errors were to decrease by a factor of 2. The absorbing properties of the natural aerosol can vary strongly, depending on the origin and the chemical composition of the particles. The spectral variability of χ for weakly absorbing aerosol particles (such as oceanic or background stratospheric aerosols) within the visible and near-infrared spectral ranges is of little importance because it would not noticeably affect the measured atmospheric transmission or the solar aureole radiances. The spectral dependence of χ for most of the moderately absorbing aerosols that have an imaginary part of the refractive index within 0.005–0.01 (i.e. dustlike, water soluble, volcanic ash) is weak and limited to the 0.001–0.002 change for wavelengths from 0.4 to 1.0 μm.[26,43] Because the spectral variability of χ is well below detectable limits, the assumption of spectrally independent aerosol refractive index appears reasonable. This assumption is also used in the vast majority of aerosol multispectral remote-sensing techniques reported in the literature.

The constant offset correction may be affected by (i) solar tracking (optical alignment) errors that are approximately independent of the alt-azimuth geometry, (ii) drive-motor errors (for example) that are dependent on the altazimuthal geometry, or (iii) nonlinearity in the phase function as a function of scan angle (see below). In any case we use this term as a catchall to eliminate all forms of systematic scanning error. If the geometry of the scan is constrained to the aureole, then it is not difficult to show that all these errors can be advantageously modeled by a simple constant offset in scattering angle (in the first approximation).

Errors that are due to inaccurate modeling of multiple scattering in the solar aureole can contribute to the errors described in Section 3. The reported accuracy of the multiple-scattering approximation of Box and Deepak[10] that we used in the study is ~2% for low aerosol loading and small scattering angles and is within 4–5% for high aerosol loading of as much as 0.4 in optical depth. These errors certainly reduce the aerosol retrieval accuracy. Box and Deepak[44] found that for aerosol optical depths less than 0.2 the errors in their multiple-scattering approximation for the solar aureole radiance generated additional errors of 2% in the derived modal radius of the particle size distribution. In this study we used only single-wavelength almucantar measurements in the inversion; thus the error estimate that we obtained can be viewed as an upper limit for the additional error in the aerosol properties retrieved from multispectral solar aureole observations of AERONET CIMEL instruments. If in our study we consider model errors as random noise, which is of course a rough assumption, and suppose that the measurement instrumental noise is equal to 5%, the total error of the aureole observations will be 6–8%; hence the more realistic estimates of retrieval accuracy would lie between those obtained for 5% and 10% aureole measurement errors (see Section 4). In spite of the relatively high model errors, the approach that employs an analytical correction for multiple-scattering effects in the solar aureole single-scattering formulation is useful; it simplifies the

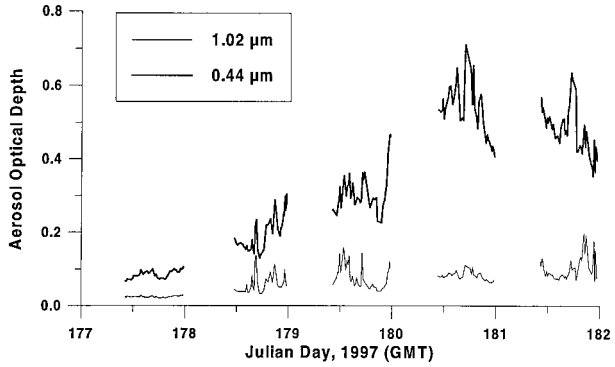

Fig. 4. Aerosol optical depth measured at Sherbrooke, Quebec (45.37 °N, 71.92 °W) from 27 June to 1 July 1997 (corresponding days of the year are 177–181).

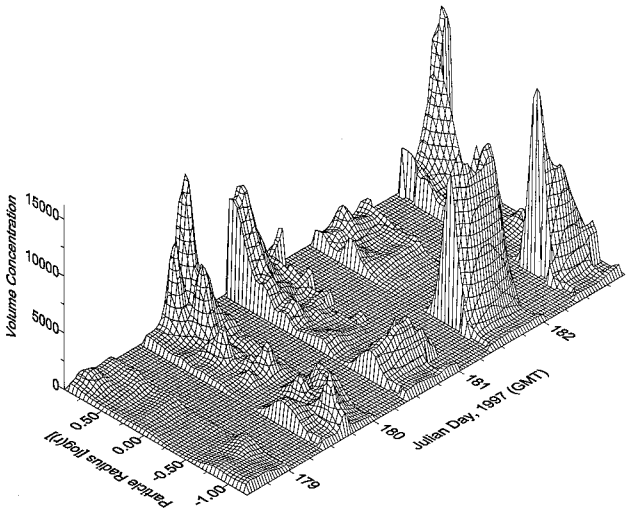

Fig. 5. Retrieved aerosol size distribution ($dV/d \ln r$) time series from 27 June to 1 July 1997 (corresponding days of the year are 177–181). Volume concentration is given in units of $(cm^3/cm^2)/\mu m \times 10^9$.

linearization of the model and allows for one-step retrieval of the aerosol's microphysical properties. There exists a certain potential to improve the analytical multiple-scattering correction model of Deepak and Box (see Ref. 25) and to enhance its accuracy. This improvement can bring additional perspectives to the application of this model to the inversion of the solar aureole data.

In principle the aerosol retrievals are functions of land surface albedo and therefore any significant deviation from the crude spectrum that we used should be investigated. However, the uncertainty in the surface reflective properties is not expected to affect the retrievals significantly. The results of the simulation study that we performed indicated that changes of the albedo within $\pm 20\%$ of the model value do not cause more than 1.5% changes in the solar aureole radiance. This additional error is significantly smaller than the measurement error.

6. Application of the Technique to Process the Sunphotometer Observation Data

Here we illustrate the performance of the retrieval scheme by applying it to CIMEL measurements made during several consecutive days (27 June–1 July 1997) at Sherbrooke, Quebec (45.37 °N, 71.92 °W). This five-day period was mostly cloud free and was characterized by significant changes in atmospheric aerosol loading. Figure 4 shows that the aerosol optical depth computed from the spectral transmission measurements was gradually increasing during the first four days and slightly decreased at the end of the fifth day of the selected period. The optical depths of Fig. 4 are reported as a function of day of the year and Greenwich Mean Time (GMT). It can be clearly seen that a ratio of the derived aerosol optical depths at the two wavelengths, 0.44 and 1.02 μm, would vary throughout the study period. This fact provides evidence that changes in the aerosol features other than a simple increase or decrease in the total particle concentration occurred and motivated a more-detailed study of the temporal behavior of the particle size distribution and refractive index.

Two AEROCAN CIMEL instruments were operating during the period of interest at Sherbrooke (numbers 81 and 84, according to the global AERONET instrument list). More than 90 almucantar and principal plane sky scans made with these two instruments during the five-day period were found to be cloud free according to the approach employed by Holben *et al.*[35] Solar aureole observations combined with almost synchronous aerosol optical depth measurements at five wavelengths (0.44, 0.50, 0.67, 0.87, and 1.02 μm) were inverted by the technique described in Sections 2–4 of this paper. The time gap between acquisition of aureole and spectral attenuation measurements did not exceed 5 min. Because of a malfunction, only the principal plane scans of CIMEL 84 were available. In the inversion procedure we used the spectral aerosol optical depth data at 1.02 μm to produce a first guess for the aerosol size distribution. The algorithm that we applied to determine the first-guess size distribution was the same as in the numerical experiments described in Section 4. The initial guess for the refractive index was set to $1.50 - i0.005$, independently of the aerosol optical depth measured.

The results presented in Fig. 5 demonstrate the variability in the aerosol particle size distribution during the period considered (note that the radius axis increases to the left). A smoothing procedure was applied to remove the excessive instability typical of the inverted size spectra. The inversion results clearly show the existence of two aerosol modes, which vary temporally in a relatively independent fashion. As can be observed, the concentration of the accumulation mode particles with radii within 0.1–0.6 μm increased during the first four days of the study period and decreased on 1 July (day 181). Obviously this mode is mainly responsible for the temporal changes in the aerosol optical depth (see Fig. 4).

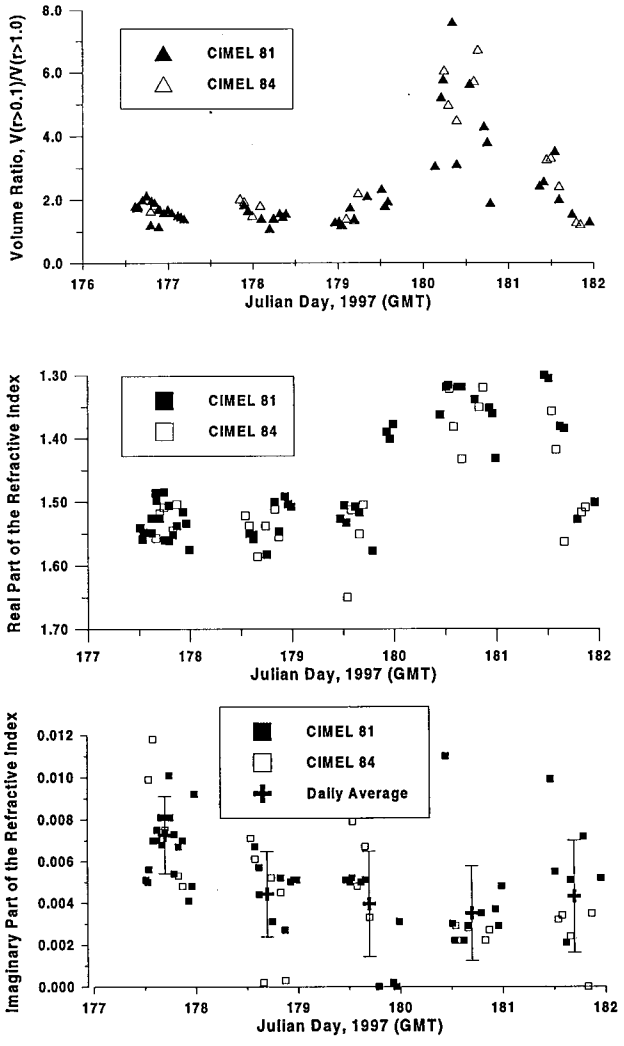

Fig. 6. Time series of the derived refractive index and the volume ratio estimated from the corresponding retrieved particle size distributions from 27 June to 1 July 1997 (corresponding days of the year are 177–181). Error bars at the bottom represent standard deviations of the daily mean values of the imaginary part of the refractive index.

The coarse mode volume concentration has two maxima: The first one was observed on the evening of 28 June (day 178), and the second one occurred on 1 July. It should be noted that a good correspondence is observed between the results of the inversion made at the end and at the beginning of consecutive days. This observation can be considered an indirect confirmation of the validity of the derived information on the aerosol size distributions.

The results of the data processing show that the retrieved value of the real part of the refractive index remained almost constant during the first three days of the observation period, with an average value of 1.53 ± 0.03 (Fig. 6). The fourth day and the first half of the last day of the observation period (days 180 and 181) reveal a significant decrease in η, to 1.30–1.40, followed by an increase to the initial values of approximately 1.50–1.56 in the evening of 1 July (day 181). Although the retrieved values of the imaginary part of the refractive index show significant scatter (Fig. 6), a significant temporal change in χ can be seen during the period in question. Over the first four days of the observation period the magnitude of the daily average χ decreased by a factor of 2 to a minimum of 0.0035 on 30 June (Julian day 180). The last day of the period of observation revealed a slight increase of $\sim$0.001 in the daily average value of the imaginary part of the refractive index. It can be observed as well that the retrievals of the real part of the refractive index from both instruments compare well. With a few exceptions the same conclusion is true with respect to the imaginary part of the refractive index. This result can be viewed as an indication of the robustness of the inversion procedure.

As was noted above, the presence of irregularly shaped aerosol particles in the atmosphere, if it is not accounted for when one is modeling aerosol radiative properties, may reveal itself through an excessive (fictitious) aerosol absorption appearing in the retrievals. The derived imaginary part of the aerosol refractive index (Fig. 6) shows no unusually high values. This result suggests that the observed aerosol particles were mostly spherical and that the possible nonsphericity effects on the retrievals could not be distinguished from other sources of variations in assumed aerosol properties.

Because the extracted particle size spectra present two independent modes that are probably of different natures and have different compositions, it is reasonable to expect changes in the refractive index with changes in the particle size distribution. To simplify the analysis we introduced another parameter to characterize the aerosol size distribution, namely, the volume ratio of aerosol particles with radii greater than 0.1 μm to particles with radii greater than 1.0 μm ($V_{0.1}/V_{1.0}$). In general, this parameter directly characterizes the importance of the total volume of the optically active aerosol particles relative to the coarse mode [or it can be viewed as an indicator of the volume ratio of the accumulation and coarse modes ($V_{0.1}/V_{1.0} = V_{0.1-1.0}/V_{1.0} + 1$)]. The results presented in Fig. 6 demonstrate a close relationship between the volume ratio and the real part of the refractive index. The increase in $V_{0.1}/V_{1.0}$ observed on days 180 and 181 indicates a significant increase in the volume of the accumulation mode particles compared with the volume of the coarse mode particles. The observed changes in the real part of the refractive index are reasonable inasmuch as the particles of the accumulation mode are predominantly the result of coagulation and condensational growth of water-soluble Aitken nuclei and in general have lower η than the dustlike particles of the aerosol coarse mode. Time changes of the imaginary part of the refractive index are on the whole consistent with the changes of the real part and with the volume ratio. Maximum values of χ ranging from 0.004 to 0.01 along with the corresponding values of η of 1.48–1.58 observed on the first day of the study period are typical for dry sulfate aerosol. The minimum in χ on

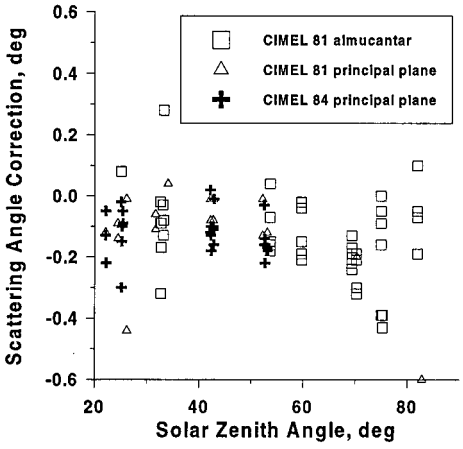

Fig. 7. Scattering angle correction factor (δ_Ω) retrieved from combined aureole and transmission measurements. Measurements used in the inversions were taken at Sherbrooke, Québec, from 27 June to 1 July 1997.

30 June (Julian day 180) corresponds to the minimum in η, which itself is close to the refractive index of water ($1.33 - i0.0$). The decrease of both real and imaginary parts of the refractive index is quite reasonable for an aerosol size distribution that is characterized by a dominant water-soluble accumulation mode. It should be noted, however, that the correlations between χ and η or between χ and $V_{0.1}/V_{1.0}$ appear to be weaker than those between η and $V_{0.1}/V_{1.0}$. This result, however, may also be related to the decreased accuracy of the χ retrieval.

To investigate the aerosol transformations during the observation period we related the derived aerosol properties to the relative-humidity data acquired at a local meteorological station located less than 15 km from the observation site. Although variations of moisture concentration are known to affect aerosol optics in the near-surface layer,[45] the derived aerosol properties were found to be practically independent of the relative humidity. Absolute values of correlation coefficients between relative humidity and the real and imaginary parts of the refractive index did not exceed 0.23. The particle size distribution as well as the refractive-index retrievals presented in Figs. 5 and 6 give no distinct indication of a meteorologically driven diurnal cycle in the aerosol size distribution or composition transformations. This means that the observed changes in the column integrated aerosol size spectra and refractive index are determined mainly by processes other than those related to the typical daily changes of the boundary-layer meteorological parameters.[46]

The retrieved values of angle correction factor δ_Ω show increased scatter (Fig. 7) for observations made at both small and large solar zenith angles. In general, the retrievals of the angular correction factor indicate a fairly high pointing precision and stability during the acquisition of aureole measurements. Only 3 of more than 90 retrievals resulted in an absolute value of δ_Ω that exceeded 0.4°. However, it is worth noting that the majority of the δ_Ω retrievals are negative; i.e., the corrected scattering angles are less than the actual observation angles. The average magnitude of the correction inferred is not high ($-0.17°$).

Inasmuch as we used measurements taken by two different instruments at different scanning geometries and at various solar zenith angles, the errors in the scattering angle mentioned above can hardly be caused by systematic pointing inaccuracies. We believe that the effect observed in the retrieved δ_Ω is the consequence of the finite instrumental field of view for the CIMEL radiometers. This effect is not taken into account in the radiative transfer model used for the data processing.

The phase function of the scattered solar radiation in the aureole range is a nonlinear function of geometrical scattering angle Ω and usually has a shape close to a power logarithm law ($\ln I_s \sim \ln \Omega$). This means that neglecting the finite dimension of the radiometer field of view will result in underestimations of the aureole radiance by the radiative transfer model. A similar effect, but of less magnitude, is caused by ignoring the finite size of the solar disk.[47] The results of the retrieval show that the inaccuracy in the aureole radiance modeling can be partially compensated for by the angular correction, i.e., by use of certain effective values of the scattering angles instead of geometrical values.

That this correction is generally negative follows if one considers that, for a given set of aerosol characteristics, a field-of-view (FOV) averaged phase function would lie slightly above its (continuous) phase function source if the former were referenced to the midpoint of each angular interval (an effect that would become less severe with increasing scattering angle). If only one corrective degree of freedom is permitted in angular dimension, then, on average, a decrease in the nominal measurement angles by a small fixed amount would better superimpose the measured (FOV averaged) phase function curve onto its modeled (aerosol-characteristics-dependent) analog.

To validate the angular correction factor value retrieved from the field observations we simulated aureole radiances computed for instruments that have an infinitely small FOV and a FOV of 1.8°. Aureole measurements for an infinitely small FOV were matched to FOV averaged measurements; i.e., the FOV averaged radiance curve was effectively shifted toward the pointwise radiance curve until the two curves were superimposed The computed shift at each scattering angle was taken as a measure of the angular correction factor. The aureole simulations for 1.8° and infinitely small instrument FOV were at the standard set of four wavelengths used by the CIMEL instrument for aureole scanning (see above) and 10 scattering angles within the 3°–16° angular range. Aerosol size distribution functions and refractive indices retrieved from field observation data were used as an input to the radiative transfer model. The angular correction factor averaged over all aure-

ole measurement simulations was $-0.15° \pm 0.02°$, which is very close to the magnitude of this factor ($-0.17°$) derived from the field aureole and transmission measurements.

Inasmuch as the solar aureole radiance is a nonlinear function of the scattering angle and wavelength, a radiance correction that would account for finite FOV effects or the effectively equivalent angular correction obviously should be wavelength and angular dependent [$\delta_\Omega = \delta_\Omega(\lambda, \Omega)$]. However, a single value of δ_Ω is sufficient to represent the first-order variation over all channels and scattering angles, and we feel justified in using this single degree of liberty.

5. Conclusions

In this paper we have reported a new technique for the simultaneous retrieval of the atmospheric aerosol particle size distribution and the refractive index from combined spectral transmission and solar aureole measurements in the visible and the near infrared. The method is based on modifications to the Mie code and incorporates computations of the derivatives of the aerosol optical properties with respect to the optical constants. The technique was used in the simulation study to examine the capabilities of the CIMEL automatic radiometers employed in the AERONET and AEROCAN networks. It also was successfully applied to monitor variations of aerosol microphysical properties derived from ground-based optical measurements performed during one particular five-day event.

It was found that the sunphotometer measurements yield the real part of the aerosol refractive index to an accuracy of 0.03–0.05 if the errors in the measurements of the aerosol optical depth and aureole radiances do not exceed 0.01 and 5%, respectively. The potential for extracting the imaginary part of the aerosol refractive index with existing ground-based sunphotometer observations is limited; only substantial changes in the absorbing properties of the aerosol, ≥ 0.004 in χ, can be effectively detected. An increase in the information content of the ground-based observations with respect to the real and the imaginary parts of the refractive index may be expected if the measurement errors are halved relative to the current levels. Such measurement accuracy may be achieved in the ground-based supersites for aerosol monitoring that are planned for construction.[37]

The technique for processing the CIMEL radiometer data was also applied to correct for possible Sunpointing and spatial positioning errors when aureole scanning measurements are performed. It was demonstrated that the values of the scattering angles employed in the aureole observations can be refined within an accuracy of 0.15°–0.19°. The small angular correction obtained indicated that CIMEL observations were largely free of significant inaccuracies in the aureole measurement angular scheme. In most cases the angular correction factor in the inversion procedure stems from the fact that the scattering angle correction can be treated as an equivalent correction to the effective sampling error in the application of discrete radiative transfer calculations to field of view and solar disk averaged aureole measurements. For the aureole scans within a 3°–16° scattering angle range it was shown that the required average angular correction has a magnitude of $-0.17°$.

Appendix A. Details of the Computations of the Derivatives of the Aerosol Optical Characteristics with Respect to the Optical Constants and the Scattering Angle

The aerosol intensity parameters $i_1(\Omega, m, r, \lambda)$ and $i_2(\Omega, m, r, \lambda)$ that determine the aerosol phase function are related to the complex scattering amplitudes S_1 and S_2:

$$i_1 = S_1 S_1^*,$$
$$i_2 = S_2 S_2^*. \tag{A1}$$

Following Deirmendjian,[20] the aerosol extinction and scattering factors as well as the scattering amplitude can be expressed in the form of infinite series:

$$Q_{\text{ext}} = 2/x^2 \sum_{n=1}^{\infty} (2n+1)\text{Re}(a_n + b_n), \tag{A2}$$

$$Q_{\text{scat}} = 2/x^2 \sum_{n=1}^{\infty} (2n+1)(|a_n|^2 + |b_n|^2); \tag{A3}$$

$$S_1 = \sum_{n=1}^{\infty} (2n+1)/[n(n+1)](a_n \pi_n + b_n \tau_n), \tag{A4}$$

$$S_2 = \sum_{n=1}^{\infty} (2n+1)/[n(n+1)](b_n \pi_n + a_n \tau_n). \tag{A5}$$

The expressions for a_n and b_n are as follows:

$$a_n = \frac{[A_n(y)/m + n/x]\text{Re}\, w_n(x) - \text{Re}\, w_{n-1}(x)}{[A_n(y)/m + n/x]w_n(x) - w_{n-1}(x)}, \tag{A6}$$

$$b_n = \frac{[A_n(y)m + n/x]\text{Re}\, w_n(x) - \text{Re}\, w_{n-1}(x)}{[A_n(y)m + n/x]w_n(x) - w_{n-1}(x)}, \tag{A7}$$

where it will be recalled that $m = \eta - i\chi, y = mx$, and $x = 2\pi r/\lambda$ is the size parameter. The coefficients π_n and τ_n are functions of only scattering angle Ω, and $w_n(x)$ are functions of only the size parameter. We can apply the following recursion formulas to compute $A_n(y)$, π_n, and τ_n:

$$A_n(y) = -n/y + [n/y - A_{n-1}(y)]^{-1}, \qquad A_0 = \cot y, \tag{A8}$$

$$\pi_n = (2n-1)/(n-1)\pi_{n-1}\cos\Omega - n/(n-1)\pi_{n-2}, \tag{A9}$$

$$\tau_n = (\pi_n - \pi_{n-2})\cos\Omega - (2n-1)\pi_{n-1}\sin^2\Omega + \tau_{n-2}, \tag{A10}$$

where

$$\pi_0 = 0, \qquad \tau_0 = 0, \qquad \pi_1 = 1,$$
$$\tau_2 = \cos\Omega, \qquad \pi_2 = 3\cos\Omega, \qquad \tau_3 = 3\cos 2\Omega.$$

In Ref. 23 the following recursion formula for computing the derivatives of $A_n(y)$ was derived through the direct differentiation of the expression [Eq. (A8)]

$$A_n'(y) = n/y^2 + [n/y^2 + A_{n-1}'(y)][n/y - A_{n-1}(y)]^{-1}.$$

The derivatives $A_n'(y)$ enter the formulation for the partial derivatives of a_n and b_n obtained by differentiation of formulas (A6) and (A7):

$$\partial a_n/\partial m = i/m^2[yA_n'(y) - A_n(y) \times \{[A_n(y)/m + n/x]w_n(x) - w_{n-1}(x)\}^2,$$

$$\partial b_n/\partial m = i[yA_n'(y) - A_n(y)] \times \{[A_n(y)m + n/x]w_n(x) - w_{n-1}(x)\}^2.$$

We can substitute the derivatives $\partial a_n/\partial m$ and $\partial b_n/\partial m$ to compute the partial derivatives of the monodispersed aerosol optical efficiency factors, scattering amplitudes, and intensity parameters with respect to the real and imaginary parts of the refractive index. We do so by applying rules for the differentiation of complex functions to formulas (A1)–(A5). For example,

$$\partial Q_{\text{ext}}/\partial\eta = 2/x^2 \sum_{n=1}^{\infty} (2n + 1)\text{Re}(\partial a_n/\partial m + \partial b_n/\partial m),$$

$$\partial S_1/\partial\eta = \sum_{n=1}^{\infty} (2n + 1)/[n(n + 1)] \times (\pi_n \text{ Re } \partial a_n/\partial m + \tau_n \text{ Re } \partial b_n/\partial m),$$

$$\partial i_1/\partial\eta = 2 \text{ Re } S_1 \text{ Re } \partial S_1/\partial\eta + 2 \text{ Im } S_1 \text{ Im } \partial S_1/\partial\eta.$$

The approach to the computations of the derivatives of the aerosol intensity parameters with respect to the scattering angles is similar to the one described above. By differentiating Eqs. (A9) and (A10) we easily obtain recursion formulas to compute the derivatives of τ_n and π_n with respect to Ω:

$$\pi_n' = (2n - 1)/(n - 1)(\pi_{n-1}' \cos\Omega - \pi_{n-1}\sin\Omega) - n/(n - 1)\pi_{n-2}',$$

$$\tau_n' = (\pi_n' - \pi_{n-2}')\cos\Omega - (\pi_n - \pi_{n-2})\sin\Omega - (2n - 1) \times (\pi_{n-1}'\sin^2\Omega + 2\pi_{n-1}\sin\Omega\cos\Omega) + \tau_{n-2}',$$

where

$$\pi_0' = 0, \quad \tau_0' = 0, \quad \pi_1' = 0, \quad \tau_2' = -\sin\Omega,$$

$$\pi_2' = -3\sin\Omega, \quad \tau_3' = -6\sin 2\Omega.$$

The expressions for the derivatives of S_1, S_2, i_1, and i_2 with respect to scattering angle Ω follow from Eqs. (A1) and (A4)–(A5) and have the same form as the expressions for the derivatives of these optical parameters with respect to the particle optical constants; for example,

$$\partial S_1/\partial\Omega = \sum_{n=1}^{\infty} (2n + 1)/[n(n + 1)](a_n\pi_n' + b_n\tau_n'),$$

$$\partial i_1/\partial\Omega = 2 \text{ Re } S_1 \text{ Re } \partial S_1/\partial\Omega + 2 \text{ Im } S_1 \text{ Im } \partial S_1/\partial\Omega.$$

Knowing the monodispersed derivatives, we can compute the derivatives of the aerosol polydispersed optical characteristics $\partial\tau_a(\lambda)/\partial\eta$, $\partial\tau_a(\lambda)/\partial\chi$, $\partial P_a(\Omega, \lambda)/\partial\eta$, $\partial P_a(\Omega, \lambda)/\partial\chi$, and $\partial P_a(\Omega, \lambda)/\partial\Omega$. in the standard way, i.e., through integration of the monodispersed characteristics with the particle size distribution.

The obvious advantage of the method developed above is that all additional computations are intimately linked to the algorithm scheme that is employed in the Mie code. Thus the derivatives of the optical characteristics with respect to the optical constants and the scattering angle are computed along with the optical characteristics themselves without a significant increase in computer time.

The authors acknowledge the support of the Canada Center for Remote Sensing (CCRS) and the Atmospheric Environment Service of Environment Canada. We thank P. Teillet of the CCRS and O. Dubovik of the AERONET group for their constructive comments.

References

1. R. J. Charlson, S. E. Schwartz, J. M. Hales, R. D. Cess, J. A. Caokley, J. E. Hansen, and D. J. Hoffman, "Climate forcing by antropogenic aerosol," Science **255,** 423–429 (1992).
2. J. A. Coakley and R. D. Cess, "Response of the NCAR community climate model to the radiative forcing by the naturally occurring tropospheric aerosols," J. Atmos. Sci. **42,** 1677–1692 (1985).
3. P. M. Teillet, G. Fedosejevs, F. J. Ahern, and R. P. Gauthier, "Sensitivity of surface reflectance retrieval to uncertainties in aerosol optical properties," Appl. Opt. **30,** 3933–3940 (1994).
4. G. E. Shaw, "Inversion of optical scattering and spectral extinction measurements to recover aerosol size spectra," Appl. Opt. **18,** 988–993 (1979).
5. N. T. O'Neill and J. R. Miller, "Combined solar aureole and solar beam extinction measurements: 2. Studies of the inferred aerosol size distribution," Appl. Opt. **23,** 3697–3703 (1984).
6. D. Tanre, C. Devaux, H. Herman, and R. Santer, "Radiative properties of desert aerosols by optical ground based measurements at solar wavelengths," J. Geophys. Res. D **93,** 14,223–14,231 (1988).
7. G. Tonna, T. Nakajima, and R. Rao, "Aerosol features retrieved from solar aureole data: a simulation study concerning a turbid atmosphere," Appl. Opt. **34,** 4486–4499 (1995).
8. T. Nakajima, G. Tonna, R. Rao, P. Boi, Y. Kaufman, and B. Holben, "Use of sky brightness measurements from ground for remote sensing of particulate polydispersions," Appl. Opt. **35,** 2672–2686 (1996).
9. M. D. King, D. M. Byrne, B. M. Herman, and J. A. Reagan, "Aerosol size distributions obtained by inversion of spectral optical depth measurements," J. Atmos. Sci. **35,** 2153–2167 (1978).
10. M. A. Box and A. Deepak, "An approximation to multiple scattering in the Earth's atmosphere: almucantar radiance formulation," J. Atmos. Sci. **38,** 1037–1048 (1981).
11. N. T. O'Neill and J. R. Miller, "Constrained linear inversion of optical scattered data for particle size spectra: an approach to angular optimization," Appl. Opt. **21,** 1231–1235 (1982).
12. T. Nakajima, M. Tanaka, and T. Yamamuchi, "Retrieval of the optical properties of the aerosols from aureole and extinction data," Appl. Opt. **22,** 2951–2959 (1983).
13. O. V. Dubovik, T. V. Lapyonok, and S. L. Oschepkov, "Im-

proved technique for data inversion: optical sizing of multicomponent aerosols," Appl. Opt. **34,** 8422–8436 (1995).
14. K. S. Shifrin, V. F. Turchin, L. S. Turovtseva, and V. A. Gashko, "Reconstruction of particles size distribution by statistical regularization of the scattered function," Izv. Atmos. Oceanic Phys. **8,** 1268–1278 (1972).
15. S. Twomey and H. B. Howell, "Some aspects of the optical estimation of microstructure in fog and cloud," Appl. Opt. **6,** 2125–2131 (1967).
16. E. R. Westwater and A. Cohen, "Application of Backus–Gilbert inversion technique to determination of aerosol size distribution from optical scattering measurements," Appl. Opt. **12,** 1340–1348 (1973).
17. J. A. Reagan, D. M. Birne, and M. D. King, "Determination of complex refractive index and size distribution of atmospheric particles from bistatic–monostatic lidar and solar radiometer measurements," J. Geophys. Res. **85,** 1591–1599 (1980).
18. M. Weindisch and W. von Hoyningen-Huene, "Possibility of refractive index determination of atmospheric aerosol particles by ground-based solar extinction and scattering measurements," Atmos. Environ. **28,** 785–792 (1994).
19. M. Tanaka, T. Nakajima, and T. Takamura, "Simultaneous determination of complex refractive index and size distribution of airborne and water-suspended particles from light scattering measurements," J. Meteorol. Soc. Jpn. **60,** 1259–1271 (1982).
20. D. Deirmendjian, *Electromagnetic Scattering on Spherical Polydispersions* (Elsevier, New York, 1969).
21. Y. J. Kaufman, A. Gitelson, A. Karnieli, E. Ganor, R. S. Fraser, T. Nakajima, S. Matoo, and B. Holben, "Size distribution and scattering phase function of aerosol particles retrieved from sky brightness measurements," J. Geophys. Res. D **99,** 10,341–10,356 (1994).
22. P. Yu. Romanov, V. V. Rozanov and Yu. M. Timofeyev, "Combined interpretation of ground-based measurement of atmospheric clarity," Izv. Akad. Sci. USSR Atmos. Oceanic Phys. **24,** 228–235 (1988).
23. V. V. Rozanov, S. P. Obrastzov, and P. Yu. Romanov, "Sensitivity of the optical characteristics of a polydispersed aerosol to variations of the complex refractive index," Izv. Akad. Sci. USSR Atmos. Oceanic Phys. **23,** 293–296 (1987).
24. J. T. Twitty, "The inversion of aureole measurements to derive aerosol size distributions," J. Atmos. Sci. **32,** 584–591 (1975).
25. Q. Jinhuan, "An approximate expression of the sky radiance in almucantar and its application," Adv. Atmos. Phys. **3,** 1–9 (1986).
26. R. A. McClatchey, H.-J. Bolle, and K. Ya. Kondratyev, "A preliminary cloudless standard atmosphere for radiation computation," Tech. Doc. 24, World Climate Programme Series WCP-112 (World Meteorological Organization, Geneva, TD-No.24 1986).
27. R. Cess and I. L. Vullis, "Inferring surface solar absorption form broadband satellite measurements," J. Clim. **2,** 974–985 (1989).
28. J. T. Houghton, F. W. Taylor, and C. D. Rodgers, *Remote Sounding of the Atmosphere* (Cambridge U. Press, Cambridge, 1984).
29. S. Twomey, "On the numerical solution of Fredholm integral equation of the first kind by the inversion of the linear system produced by quadrature," J. Assoc. Comput. Mach. **10,** 97–101 (1963).
30. D. Q. Wark and H. E. Fleming, "Indirect measurements of atmospheric temperature profiles from satellites. I. Introduction," Mon. Weather Rev. **94,** 351–362 (1966).
31. V. F. Turchin and V. Z. Nozik, "Statistical regularization of the solution of incorrectly posed problems," Izv. Atmos. Ocean. Phys. **5,** 29–38 (1969).
32. E. R. Westwater and O. N. Strand, "Statistical information content of radiation measurements used in indirect sensing," J. Atmos. Sci. **25,** 750–758 (1968).
33. C. D. Rodgers, "Statistical principles of inversion theory," in *Inversion Methods in Atmospheric Remote Sounding*, A. Deepak, ed. (Academic, New York, 1977), pp. 117–134.
34. L. A. Remer, S. Gasso, D. A. Hegg, Y. J. Kaufman, and B. N. Holben, "Urban/industrial aerosol: ground-based sun/sky radiometer and airborne *in situ* measurements," J. Geophys. Res. D **102,** 16,849–16,859 (1997).
35. B. Holben, T. Eck, I. Slutsker, D. Tanré, J. P. Buis, A. Setzer, E. Vermote, J. A. Reagan, Y. J. Kaufman, T. Nakajima, F. Lavenu, I. Janovak, and A. Smirnov, "Automatic sun and sky scanning radiometer system for network aerosol monitoring," Remote Sens. Environ. **66,** 1–16 (1998).
36. N. T. O'Neill, A. Royer, P. Romanov, P. M. Teillet, and B. McArthur, "The AEROCAN sunphotometer network: a component of a cal/val strategy for consistent image correction," in *Proceedings of the Twentieth Canadian Symposium on Remote Sensing: Geomatics in the Era of Radarsat*, available on a 1997 CD-ROM from National Defence Headquarters, Directorate of Geographic Operations, Ottawa, Ontario K1A 0K2, Canada.
37. Y. J. Kaufman, D. Tanre, H. R. Gordon, T. Nakajima, J. Lenoble, R. Frouin, H. Grassl, B. M. Herman, M. D. King, and P. M. Teillet, "Passive remote sensing of tropospheric aerosol and atmospheric correction for the aerosol effect," J. Geophys. Res. D **102,** 16,815–16,830 (1997).
38. M. I. Mishchenko, L. D. Travis, R. A. Kahn, and R. A. West, "Modeling phase functions for dustlike tropospheric aerosols using a shape mixture of randomly oriented polydispersed spheroids," J. Geophys. Res. D **102,** 16,831–16,847 (1997).
39. J. B. Pollack and J. N. Cuzzy, "Scattering by nonspherical particles of size comparable to a wavelength: a new semi-empirical theory and its application to tropospheric aerosols," J. Atmos. Sci. **37,** 868–881 (1980).
40. P. Koepke and M. Hess, "Scattering functions of tropospheric aerosol: the effects of nonspherical particles," Appl. Opt. **27,** 2422–2430 (1988).
41. T. Nakajima, M. Tanaka, M. Yamano, M. Shiobara, K. Arao, and Y. Nakanishi, "Aerosol optical characteristics in the yellow sand events observed in May, 1982 at Nakasaki. II. Models," J. Meteorol. Soc. Jpn. **67,** 279–291 (1989).
42. R. G. Pinnick, D. E. Carroll, and D. J. Hoffman, "Polarized light scattered from monodisperse randomly oriented nonspherical aerosols: measurements," Appl. Opt. **15,** 384–393 (1976).
43. G. A. d'Almeida, P. Koepke, and E. P. Shettle, *Atmospheric Aerosols: Their Global Climatology and Radiative Characteristics* (Deepak, Hampton, Va., 1991).
44. M. A. Box and A. Deepak, "Retrieval of aerosol size distributions by inversion of simulated aureole data in the presence of multiple scattering," Appl. Opt. **18,** 1376–1382 (1979).
45. R. M. Hoff, L. Guise-Bagley, R. M. Staebler, H. A. Wiebe, J. Brook, B. Georgi, and T. Dusterdiek, "Lidar, nephelometer, and *in situ* aerosol experiments in southern Ontario," J. Geophys. Res. D **101,** 19,199–19209 (1996).
46. N. T. O'Neill, A. Royer, P. Coté, and B. McArthur, "Relations between optically derived aerosol parameters, humidity, and air-quality data in an urban atmosphere," J. Appl. Meteorol. **32,** 1484–1498 (1993).
47. M. A. Box and A. Deepak, "Finite sun effects in the interpretation of solar aureole," Appl. Opt. **20,** 2806–2810 (1981).